Carbohydrate Polymers 84 (2011) 770–774

Contents lists available at ScienceDirect

Carbohydrate Polymers

journal homepage: www.elsevier.com/locate/carbpol

Core–shell silica@chitosan nanoparticles and hollow chitosan nanospheres using silica nanoparticles as templates: Preparation and ultrasound bubble application

Ying-Ling Liu[a,*], Yen-Hsing Wu[a], Wei-Bor Tsai[b], Chih-Chi Tsai[b], Wen-Shiang Chen[c], Chuan-Shao Wu[d]

[a] Department of Chemical Engineering and R&D Center for Membrane Technology, Chung Yuan Christian University, #200 Chung-Pei Road, Chungli, Taoyuan 32023, Taiwan
[b] Department of Chemical Engineering, National Taiwan University, Taipei 10617, Taiwan
[c] Department of Physical Medicine and Rehabilitation and National Taiwan University Hospital, National Taiwan University, Taipei 10617, Taiwan
[d] Department of Materials and Fiber, Nanya Institute of Technology, Chungli, Taoyuan 320, Taiwan

ARTICLE INFO

Article history:
Received 23 September 2009
Received in revised form 6 February 2010
Accepted 19 March 2010
Available online 27 March 2010

Keywords:
Nanoparticles
Chitosan
Hollow nanosphere
Ultrasound image

ABSTRACT

This work reports the preparation of chitosan hollow nanospheres and their uses as the ultrasound-induced imaging agents. Reaction of chitosan to the 4-isocyanato-4′-(3,3-dimethyl-2,4-dioxo-azetidino)diphenylmethane modified silica nanoparticles forms silica@chitosan core shell nanoparticles. Removal of the silica cores with hydrofluoride generates the chitosan hollow nanospheres. Structures and morphology of the silica@chitosan core–shell nanoparticles and chitosan hollow nanospheres are characterized with an X-ray photoelectron spectroscopy and electron microscopies. Moreover, perfluoropentane is used an imaging gas to be filled into the chitosan hollow nanospheres. The gas-filled chitosan hollow nanospheres show ultrasonic-induced imaging behavior, demonstrating their potentials of applications in ultrasound-induced image.

1. Introduction

Gene delivery plays an important role in gene therapy. Concerning the safety and operation convenience of the gene delivers, the researches trend to using non-viral delivers to replace viral vectors (Ghosh, Kim, Han, Forbes, & Rotello, 2008; Green et al., 2008; Luo & Stalzman, 2000; Strand, Danielsen, Christiansen, & Varum, 2005; Takahashi, Hirose, Kojima, Harada, & Kono, 2007; Zhang et al., 2008). Organic and inorganic nanoparticles are the most studied candidates of the non-viral delivers. The transfection efficiency of the non-viral systems is not comparable to the efficiency of the viral delivers (Kodama, Katayama, Shoji, & Nakashima, 2006; Strand et al., 2005). Therefore, the relatively high transfection efficiency of the gas-filled microbubbles is noteworthy (Cavalier et al., 2008; Cheng, Xia, & Chan, 2004; Lentacker et al., 2006; Marmottant & Hilgenfeldt, 2003; Mehier-Humbert, Bettinger, Yan, & Gyu (2005); Mehier-Humbert et al., 2007; Suzuki et al., 2007; Taniyama et al., 2002). The gas-filled microbubbles are ultrasound contrast particles for molecular imaging (Klibanov, 2005), which can be utilized in gene delivery through the ultrasound-induced cavitation technique. The gas-filled bubbles should have sizes smaller than red blood cells for intravascular applications (Cavalier et al., 2008; Suzuki et al., 2007), and are easily decorated with other materials. One example is the liposome bubbles. Gas-filled liposome bubbles together with the ultrasound-induced cavitation technique show high efficiency in gene delivery (Suzuki et al., 2007). However, the stability of the bubble liposomes is not satisfied. To improve the stability of microbubbles, Cavalier et al. (2008) reported the cross-linked poly(vinyl alcohol) (PVA) microbubbles using NO as an imaging gas. There still was some space to reduce the sizes of the PVA bubbles.

The bubble systems need size reduction to be sub-micrometers and high stability. Chitosan is a nature polysaccharide. Chitosan has some attractive characteristics, such as low price, biocompatibility, hydrophilicity, moderate mechanical property, and chemical versatility, for uses gene and drug delivery. The hollow spheres of chitosan have received research attentions for drug delivery. Hollow chitosan spheres can be prepared using inorganic nanoparticles as sacrificial templates. One example is removal of AgCl cores from AgCl@polypyrrole–chitosan core–shell nanoparticles to obtain the corresponding polypyrrole–chitosan hollow nanospheres (Cheng et al., 2004). Hu et al. (2005) reported a core-template free approach to prepare chitosan/poly(acrylic acid) (PAA) hollow nanospheres. The applications of the chitosan/PAA hollow nanospheres as drug carriers were also studied (Hu et al., 2007). Qian, Zhang, Li, Liu, & Hu (2008) prepared chitosan hollow microspheres using carboxyl-functionalized polystyrene (PS-COOH) particles as templates. Chitosan shell absorbed onto PS-COOH particle surfaces through electrovalent interaction. Removal of the PS cores with tetrahydrofuran (THF) resulted in the corresponding chitosan hol-

* Corresponding author. Tel.: +886 3 2654130; fax: +886 3 2654199.
E-mail addresses: ylliu@cycu.edu.tw, yingliu.tw@yahoo.com.tw (Y.-L. Liu).

0144-8617/$ – see front matter © 2010 Elsevier Ltd. All rights reserved.
doi:10.1016/j.carbpol.2010.03.033

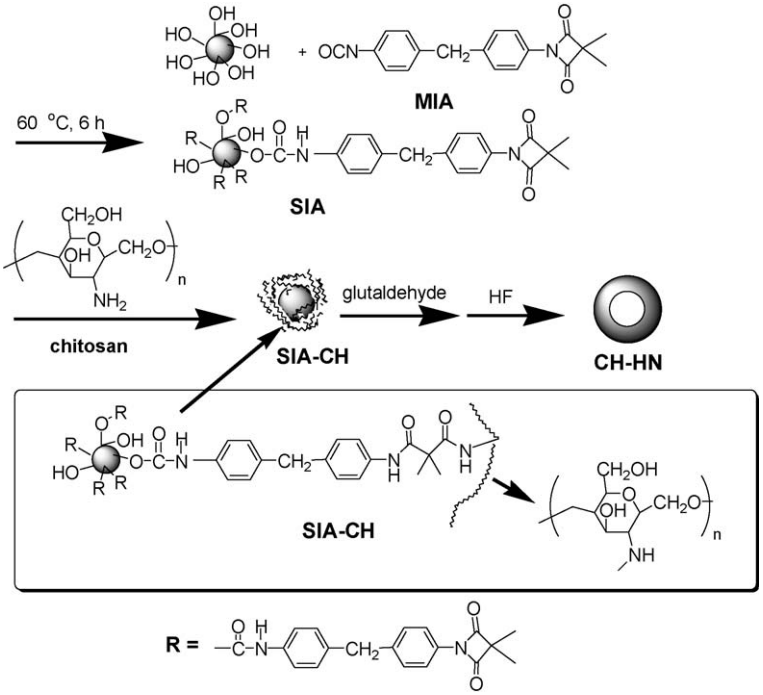

Fig. 1. Preparation of core–shell silica@chitosan nanoparticles (SIA-CH) and chitosan hollow nanospheres (CH-HN).

low spheres. However, to our best knowledge, the uses of chitosan hollow spheres as ultrasound-induced imaging bubbles are not studied.

In this work we report the preparation of chitosan hollow spheres and explore the uses of the chitosan hollow spheres as bubble agents in the ultrasound imaging techniques. The preparation of chitosan hollow spheres includes surface-functionalization of silica nanoparticles (SNPs), reaction of chitosan to the functionalized SNPs, cross-linking the chitosan shell layer, and removal of the silica cores with hydrofluoride (Fu, Shang, Hong, Kang, & Neoh, 2005a; Fu, Shang, Hong, Kang, & Neoh, 2005b; Fu, Zhao, Sun, Kang, & Neoh, 2007). Perfluoropentane is used an imaging gas to be filled into the chitosan hollow spheres. The gas-filled chitosan hollow nanospheres demonstrate the ultrasonic-induced imaging behavior, indicating their potentials of applications for gene delivery with the ultrasound-induced cavitation technique.

2. Experimental

2.1. Materials

Chitosan (85% of deacetylation) was received from Sigma chemical Co. Nanoscale silica particles were purchased from Nissan Chemical Co., Japan. The commercial product of MIBK-ST, in which 30 wt% of silica (particle size: 10–20 nm) was dispersed in methylisobutylketone (MIBK), was used. 4-Isocyanato-4′-(3,3-dimethyl-2,4-dioxo-azetidino)diphenylmethane (MIA) was prepared in our laboratory according to the reported method (Chen, Dai, Chang, Su, & Jeng, 2005). Glutaraldehyde from Acros was used as a cross-linking agent for chitosan. Perfluoropentane was purchased from Jing-He Science Co., Ltd. (Taoyuan, Taiwan). SonoVue® BR from Bracco Co. (Milan, Italy) was used for a control test of ultrasound-induced imaging.

2.2. Characterization

FTIR spectra were recorded with a Perkin-Elmer spectrum One FTIR. X-ray photoelectron spectroscopy (XPS) analysis was conducted with using a VG MICROTECH MT-500 ESCA (British) using a Mg Kα line as a radiation source. Transmission electron micrographs were taken with a Hitachi H-7500 TEM. The specimens were deposited onto copper grid directly from suspension. Scanning electron micrographs (SEM) were obtained with a Hitachi S-4800 field-emission SEM. Thermogravimetric analysis (TGA) was performed with an instrument from Thermal Analysis Incorporation (TA-TGA 2050) at a heating rate of 10 °C/min under nitrogen atmosphere. The sizes of nanoparticles were measured with a particle analyzer of Zetasizer Nano ZEN3600, Malvern Instrument, UK. A 633 nm laser was fitted to the instrument.

2.3. Preparation of core–shell silica@chitosan nanospheres

MIA modified silica nanoparticles (SIA) with a MIA content of about 30 wt% was prepared in the laboratory according to the reported method (Liu, Wu, Jeng, & Dai, 2009). MIBK-ST (9.0 g) and MIA (1.1 g) were put into a 15 mL round-bottom flask. After reaction at 60 °C for 6 h under a dry nitrogen atmosphere, silica nanoparticles were collected with a centrifuge (13,000 rpm) and dried under vacuum at 30 °C for 3 h. SIA was obtained with a yield of 81 wt%.

Chitosan was dissolved in an 1 wt% acetic acid aqueous solution to prepare a chitosan solution of 1.5 wt%. SIA (0.3 g) was added into the chitosan solution (50 mL). After being treated with an ultrasonic bath for 15 min, the solution was reacted at 60 °C for 6 h. Silica nanoparticles collected with a centrifuge (13,000 rpm) were redispersed in acetic aqueous solution and collected again to remove out the physically absorbed chitosan. After drying at 30 °C under a reduced pressure, core–shell silica@chitosan nanospheres (SIA-CH) were obtained (0.22 g).

2.4. Preparation of chitosan hollow nanoparticles

SIA-CH (0.2 g) was dispersed in glutaraldehyde at 30 °C for 24 h to cross-link the shell chitosan layer. The collected cross-linked SIA-CH was dispersed in a hydrofluoride aqueous solution (1 wt%) to remove out the silica cores of the SIA-CH nanoparticles. The nanoparticles were then collected with a centrifuge, washed with

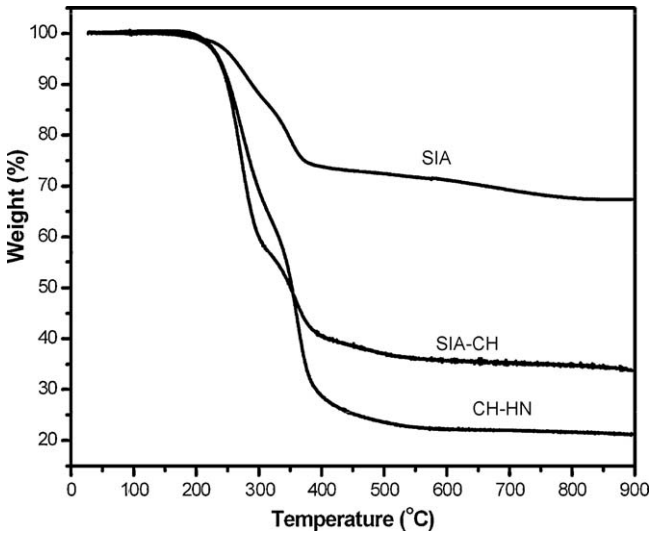

Fig. 2. TGA thermograms of the prepared nanoparticles SIA, SIA-CH, and CH-HN.

distilled water, and dried at 30 °C under vacuum to result in the chitosan hollow nanospheres (CH-HN, 0.13 g).

2.5. Ultrasound imaging in vitro

Chitosan hollow nanospheres (CH-HN) were charged into an 8-ml tube. The tube was then sealed and vacuumed. Liquid-form perfluoropentane (0.6 ml) was added to the tube and allowed to vaporize at 40 °C. After addition of phosphate buffered saline (PBS), the particle-contained liquid was transferred into a phantom for ultrasound detection (Lafon et al., 2005). The probe (L38/10–5 MHz) of a high resolution ultrasound system (Titan®, SonoSite, Bothel, WA, USA) was positioned next to the phantom and the bubbles were imaged. Commercially available ultrasound agent suspension, SonoVue®, was used for the control test.

3. Results and discussion

3.1. Preparation of chitosan hollow nanosphere

MIA possesses two functional groups, one is isocyanate and the other one is azetidine-2,4-dione. The isocyanate groups of MIA are highly reactive toward the silanol groups of SNPs. MIA molecules can decorate to the surfaces of SNPs through the reaction between isocyanate and silanol groups. The MIA-modified SNPs (SIA) possess azetidine-2,4-dione groups, which are highly selective and reactive toward primary amine groups (Chen et al., 2005). Therefore, chitosan, which possesses side primary amine groups, could react onto SIA through the reaction between the azetidine-2,4-dione groups of SIA and the amine groups of chitosan. The obtained nanoparticles have chitosan shells and SNP cores, i.e. the core–shell silica@chitosan nanoparticles (SIA-CH). After cross-linking the chitosan shell of SIA-CH with glutaraldehyde and removal of their silica cores with HF treatment, we obtained the corresponding chitosan hollow nanospheres (CH-HN) (Fig. 1).

SIA exhibits a weight loss of about 25 wt% in thermogravimetric analysis because of the degradation of the organic MIA portion. Meanwhile, SIA-CH exhibits a 65 wt% loss in its TGA thermogram (Fig. 2). The increase in the weight loss originates from the chitosan shell layer, indicating the success of chitosan incorporation to SIA. The weight ratio of silica core to organic shell is 35/65 (about 0.54) for SIA-CH. The weight fractions of silica core, MIA, and chitosan in SIA are about 35, 12, and 53%, respectively. The two-stage weight loss of SIA-CH is noteworthy. The first stage of weight loss appeared

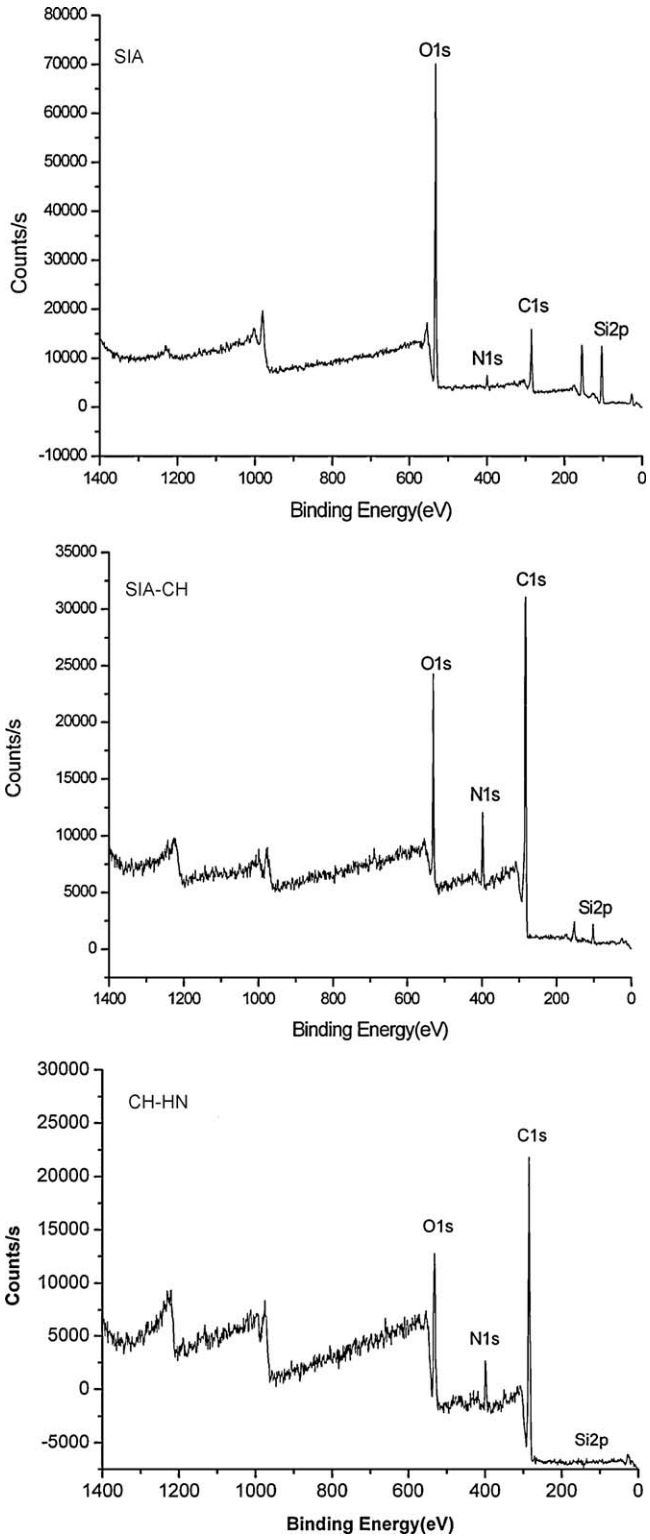

Fig. 3. XPS spectra of the prepared nanoparticles SIA, SIA-CH, and CH-HN.

at 220–300 °C and the other one did at 300–400 °C. As SIA showed a major weight loss at about 270–350 °C, the first-stage weight loss observed with SIA-CH comes from the degradation of chitosan portion and the second-stage from the MIA degradation. The thermal degradation behavior of the chitosan hollow nanospheres was similar to that observed with SIA-CH, as they possessed similar organic portions. The degradation temperatures of CH-HN shift to higher temperatures because the cross-linked structure of chitosan in CH-

Table 1
XPS elemental analysis on the nanoparticles SIA, SIA-CH, and CH-HN.

Samples	O (%)	N (%)	C (%)	Si (%)
SIA	30.4	1.2	16.7	51.2
SIA-CH	14.4	7.9	70.9	6.7
CH-HN	13.3	7.1	78.3	1.3

HN. In addition, the char yield of CH-HN is about 20 wt%, which is smaller than that observed with SIA-CH (35 wt%). The decrease in the char yield indicates the decreases in the silica portion and the removal of silica cores from SIA-CH. Removal of silica cores consequently transforms the core–shell silica@chitosan nanoparticles to be the chitosan hollow nanospheres. However, the removal of silica core might not be completed. In addition, the FTIR analytical results give additional supports to the removal of silica cores of SIA-CH and formation of CH-HN hollow nanospheres. The peak intensities of the silica absorptions at about 1095 cm^{-1} for SIA-CH and CH-HN decrease with HF treatments (figure not shown). XPS analysis data also support to the chemical structures of the nanoparticles. As shown in Fig. 3, besides O and Si signals, SIA also exhibited C_{1s} and N_{1s} signals at about 400 and 264 eV, respectively due to the presence of MIA moieties. The incorporation of chitosan to SIA resulted in the elemental content increases from 1.2 to 7.9% for nitrogen and from 16.7 to 70.9% for carbon (Table 1). Meanwhile, the measured Si content decreased from 51.7% of SIA to 6.7% of SIA-CH with chitosan incorporation. The Si content of CH-HN further decreased to 1.3% due to the removal of silica with HF. Removal of silica from SIA-CH also results in an increase in the carbon content from 70.9 to 78.3%. Meanwhile, the no obvious changes appear with the nitrogen contents of SIA-CH (7.9%) and CH-HN (7.1%) (Table 1).

Fig. 4 shows the micrographs of SIA-CH core–shell particles and the corresponding chitosan hollow nanospheres CH-HN. The particle sizes of SIA-CH are about 180 nm in SEM micrographs. The particle size of SIA-CH is close to the value (200 nm) read from the light scattering measurement. The core shell structure of SIA-CH is not clear in the SEM micrographs, but appears in the TEM micrographs. As shown in Fig. 4C, the dark portion presents the silica core and the corona portion the polymer shell, as silicon has a relatively high electron contrast in TEM observation. After HF treatment, CH-HN particles show hollow structures in both SEM and TEM micrographs. HF treatments remove out the silica cores of SIA-CH and do not obviously change the particle sizes.

3.2. Chitosan hollow nanosphere mediated ultrasound-induced images

The application potential of the chitosan hollow nanospheres in ultrasound imaging techniques and ultrasound-induced cavitation gene delivery is examined by an ultrasound-induced imaging test with perfluoropentane as an imaging gas. Previously, Suzuki et al. (2007) utilized bubble liposomes for the ultrasound-induced cavitation gene delivery. In their study, sonication of the liposomes under high pressure with the fluorocarbon gas is the critical step in the preparation of liposome bubble imaging agents. However, one advantage of the chitosan hollow spheres is that perfluoropentane could fill the chitosan hollow nanospheres without any sonication or shaking. As shown in Fig. 5, chitosan nanoparticles without perfluoropentane infusion did not induce any cloudy ultrasonographic image. On the other hand, the ultrasonographic image of chitosan hollow nanosphere suspension infused with perfluoropentane became cloudier, similar to that observed with the control test using SonoVue® BR as an agent. The ultrasound-induced images appeared with the chitosan hollow spheres confirm that the chitosan hollow nanospheres trap perfluoropentane gas and the gas-infused chitosan hollow nanospheres could demonstrate the ultrasound imaging property. Further studies are under investigation to optimize the preparation conditions of CH-HN and to perform the ultrasound-induced cavitation gene delivery.

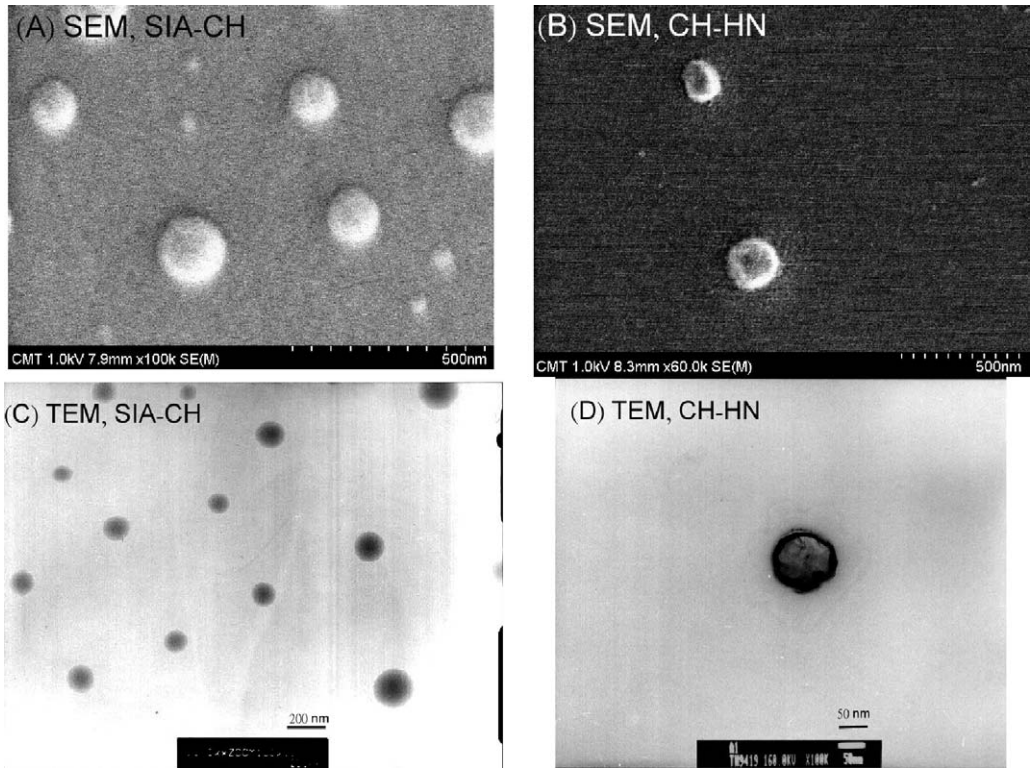

Fig. 4. SEM micrographs of SIA-CH (A) and CH-HN (B); TEM micrographs of SIA-CH (C) and CH-HN (D).

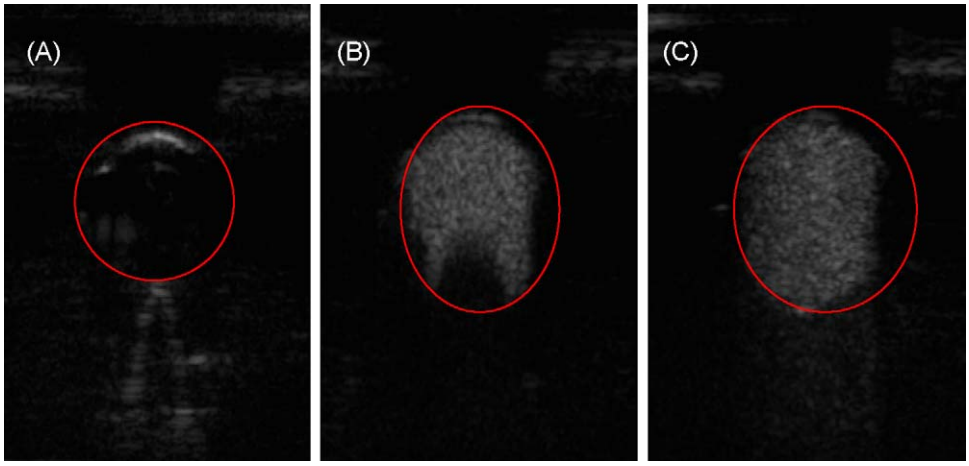

Fig. 5. The ultrasonographic images of (A) chitosan nanoparticles without perfluoropentane infusion, (B) SonoVue®, and (C) the chitosan hollow nanospheres infused with perfluoropentane. The ultrasonographic images of PBS solution and the liquid-form perfluoropentane alone were the same as (A).

4. Summary

In this work we report a facile approach to prepare silica@chitosan core–shell nanoparticles and the corresponding chitosan hollow nanospheres. The preparation route is effective for other polymeric hollow nanospheres made of polymers with primary amine groups. With perfluoropentane as an imaging gas, the gas-filled chitosan hollow nanospheres demonstrate the ultrasonic-induced imaging behavior, showing their application potentials in ultrasound images and gene delivery.

Acknowledgements

Financial support on this work from the Center-of-Excellence (COE) Program on Membrane Technology from the Ministry of Education (MOE), Taiwan and from the Project Toward Sustainable Green Technology in the Chung Yuan Christian University, Taiwan (grant CYCU-98-CR-CE) is appreciated.

References

Cavalier, F., Finelli, I., Tortora, M., Mozetic, P., Chiessi, E., Polizio, F., et al. (2008). Polymer micribubbles as diagnostic and therapeutic gas delivery device. *Chemistry of Materials*, *20*, 3254–3258.

Chen, J. P., Dai, S. A., Chang, H. L., Su, W. C., & Jeng, R. J. (2005). Facile approach to polyurea/malonamide dendrons via a selective ring-opening addition reaction of azetidine-2,4-dione. *Journal of Polymer Science Part A: Polymer Chemistry*, *43*, 682–688.

Cheng, D., Xia, H., & Chan, H. S. O. (2004). Facile fabrication of AgCl@polypyrrole–chitosan core–shell nanoparticles and polymeric hollow nanospheres. *Langmuir*, *20*, 9909–9912.

Fu, G. D., Shang, Z., Hong, L., Kang, E. T., & Neoh, K. G. (2005a). Preparation of cross-linked polystyrene hollow nanospheres via surface-initiated atom transfer radical polymerization. *Macromolecules*, *38*, 7867–7871.

Fu, G. D., Shang, Z., Hong, L., Kang, E. T., & Neoh, K. G. (2005b). Nanoporous, ultralow-dielectric-constant fluoropolymer films from agglomerated and crosslinked hollow nanospheres of poly(pentafluorostyrene)-block-poly(divinylbenzene). *Advanced Materials*, *17*, 2622–2626.

Fu, G. D., Zhao, J. P., Sun, Y. M., Kang, E. T., & Neoh, K. G. (2007). Conductive hollow nanospheres of polyaniline via surface-initiated atom transfer radical polymerization of 4-vinylaniline and oxidative graft copolymerization of aniline. *Macromolecules*, *40*, 2271–2275.

Ghosh, P. S., Kim, C. K., Han, G., Forbes, N. S., & Rotello, V. M. (2008). Efficient gene delivery vectors by tuning the surface charge density of amino acid-functionalized gold nanoparticles. *ACS Nano*, *2*, 2213–2218.

Green, J. J., Zhou, B. Y., Mitalipova, M. M., Beard, C., Langer, R., Jaenisch, R., et al. (2008). Nanoparticles for gene transfer to human embryonic stem cell colonies. *Nano Letters*, *8*, 3126–3130.

Hu, Y., Chen, Y., Chen, Q., Zhang, L., Jiang, Z., & Yang, C. (2005). Synthesis and stimuli-responsive properties of chitosan/poly(acrylic acid) hollow nanospheres. *Polymer*, *46*, 12703–12710.

Hu, Y., Ding, Y., Ding, D., Sun, M., Zhang, L., Jinag, X., et al. (2007). Hollow chitosan/poly(acrylic acid) nanospheres as drug carriers. *Biomacromolecules*, *8*, 1069–1076.

Klibanov, A. L. (2005). Ligand-carrying gas-filled microbubbles: ultrasound contrast agents for targeted molecular imaging. *Bioconjugate Chemistry*, *16*, 9–17.

Kodama, K., Katayama, Y., Shoji, Y., & Nakashima, H. (2006). The features and shortcomings for gene delivery of current non-viral carriers. *Current Medicinal Chemistry*, *13*, 2155–2161.

Lafon, C., Zderic, V., Noble, M. L., Yuen, J. C., Kaczkowski, P. J., Sapozhnikov, O. A., et al. (2005). Gel phantom for use in high-intensity focused ultrasound dosimetry. *Ultrasound in Medicine and Biology*, *31*, 1383–1389.

Lentacker, I., De Geest, B. D., Vandenbroucke, R. E., Peeters, L., Demeester, J., De Smedt, S. C., et al. (2006). Ultrasound-responsive polymer-coated microbubbles that bind and protect DNA. *Langmuir*, *22*, 7273–7278.

Liu, Y. L., Wu, Y. H., Jeng, R. J., & Dai, S. A. (2009). Functionalization of silica nanoparticles with 4-isocyanato-4′-(3,3′-dimethyl-2,4-dioxo-azetidino)diphenyl methane, surface chemical reactivity and nanohybrid preparation. *Journal of Colloids and Interface Science*, *336*, 189–194.

Luo, D., & Stalzman, W. M. (2000). Synthetic DNA delivery systems. *Nature Biotechnology*, *18*, 33–37.

Marmottant, P., & Hilgenfeldt, S. (2003). Organic chemistry: molecular diversity by design. *Nature*, *423*, 153–154.

Mehier-Humbert, S., Bettinger, T., Yan, F., & Gyu, R. H. (2005). Plasma membrane poration induced by ultrasound exposure: implication for drug delivery. *Journal of Controlled Release*, *104*, 213–222.

Mehier-Humbert, S., Yang, F., Frinking, P., Schneider, M., Gyu, R. H., & Bettinger, T. (2007). Ultrasound-mediated gene delivery: influence of contrast agent on transfection. *Bioconjugate Chemistry*, *18*, 652–662.

Strand, S. P., Danielsen, S., Christiansen, B. E., & Varum, K. M. (2005). Influence of chitosan structure on the formation and stability of DNA–chitosan polyelectrolyte complexes. *Biomacromolecules*, *6*, 3357–3366.

Suzuki, R., Takizawa, T., Negishi, Y., Hagisawa, K., Tanaka, K., Sawamura, K., et al. (2007). Gene delivery by combination of novel liposomal bubbles with perfluoropropane and ultrasound. *Journal of Controlled Release*, *117*, 130–136.

Takahashi, T., Hirose, J., Kojima, C., Harada, A., & Kono, K. (2007). Synthesis of poly(amidoamine) dendron-bearing lipids with poly(ethylene glycol) grafts and their use for stabilization of nonviral gene vectors. *Bioconjugate Chemistry*, *18*, 1163–1169.

Taniyama, Y., Tachibana, K., Hiraoka, K., Aoki, M., Yamamoto, S., Matsumoto, K., et al. (2002). Development of safe and efficient novel nonviral gene transfer using ultrasound: enhancement of transfection efficiency of naked plasmid DNA in skeletal muscle. *Gene Therapy*, *9*, 372–380.

Qian, Z., Zhang, Z., Li, H., Liu, H., & Hu, Z. (2008). Facile preparation of monodisperse hollow cross-linked chitosan microspheres. *Journal of Polymer Science Part A: Polymer Chemistry*, *46*, 228–237.

Zhang, X., Sharma, K. K., Boeglin, M., Ogier, J., Mainard, D., Voegel, J. C., et al. (2008). Transfection ability and intracellular DNA pathway of nanostructured gene-delivery systems. *Nano Letters*, *8*, 2342–2346.